Available online at www.sciencedirect.com
SCIENCE DIRECT•
Mathematical and Computer Modelling 40 (2004) 1075–1087
MATHEMATICAL AND COMPUTER MODELLING
www.elsevier.com/locate/mcm

Nonlinear Uncertainty Model of a Magnetic Suspension System

O. AGAMENNONI
Dept. de Ing. Eléctrica y de Computadoras
Universidad Nacional del Sur, Argentina
and
C.I.C. Comisión de Investigaciones Cientificas
Buenos Aires, Argentina

I. ŠKRJANC AND M. LEPETIC
Faculty of Electric Engineering
University of Ljubljana, Slovenia

H. CHIACCHIARINI
Dept. de Ing. Eléctrica y de Computadoras
Universidad Nacional del Sur, Argentina
and
CONICET (Consejo Nacional de Investigaciones Científicas y Técnicas)

D. MATKO
Faculty of Electric Engineering
University of Ljubljana, Slovenia

(Received June 2003; revised and accepted September 2003)

Abstract—The nonlinear identification of a nominal model as well as the uncertainty bounds of a magnetic suspension system is developed. This system has a nonsymmetric dynamic behavior; it has an undershoot but not an overshoot. The proposed model structure is a cascade of a global linear fuzzy dynamic block followed by a piecewise linear function. This model structure allows a proper identification of the system dynamic and a tight description of the uncertainties.

Keywords—Nonlinear systems identification, Uncertain systems, Fuzzy logic, Piecewise linear functions.

1. INTRODUCTION

The identification of nonlinear systems from input output data is a very important subject in many different technological areas, like control system design. A nonlinear model can properly describe the dynamic behavior of the system over a large operating region. One of the main problems in nonlinear system identification is the evaluation of a proper model structure. Robust

This work has been done in the frame of Bilateral Argentinian Slovene project between Universidad Nacional del Sur, Bahía Blanca and Faculty of Electrical Engineering, Ljubljana, entitled: Human resources improvements in system analysis and control.

0895-7177/04/$ - see front matter Typeset by $\mathcal{A}_{\mathcal{M}}\mathcal{S}$-TEX
doi:10.1016/j.mcm.2003.09.043

control theory has motivated developments of new model structures to achieve tight uncertainty description. However, the complexity of the robust stability and performance analysis problem strongly depends on the uncertainty model. Considerable efforts have been carried out in this area, specially since the advent of neural networks and fuzzy logic techniques [1]. In the case of fading memory system, Wiener like models help to solve the trade-off between simplicity of the robust stability analysis and quality of the representation. The Wiener model is composed by a linear dynamic block based on a Laguerre basis transfer functions followed by an Hermite polynomial. From the original structure many other approaches have been developed using different linear dynamic representation [2], like Kautz series [3] and wavelet transfer functions [4,5], as well as different nonlinear approximation approaches like Neural Networks [6,7].

In this paper, the nonlinear nominal as well as the uncertainty model evaluation problem of a stabilized magnetic suspension system from input output experimental data is considered. The system exhibits a particular behavior; an undershoot when the reference signal is going down. Global linear fuzzy models have proved to be an effective tool to approximate the main dynamic response of the system [8]. A piecewise linear (PWL) function approximation technique is used [9] to closely describe the nonlinearities as well as the model uncertainty. The final model structure resembles a Wiener structure where the fuzzy model describe the dynamic and the PWL function the static gain. The PWL function approximation allows the evaluation of upper an lower bounds of the static nonlinear gain. These bounds may be used to describe the dynamic model uncertainty. One of the main advantages of this function approximation technique is the simplicity of the electronic VLSI implementation [9]. Then efficient model implementations may be achieved for a large class of applications.

The paper is organized as follows. Section 2 describes the magnetic suspension system. Section 3 presents the model structure used. In Section 4, the modelling results are discussed. Finally, in Section 5, some concluding remarks are presented.

2. MAGNETIC SUSPENSION SYSTEM

The magnetic suspension system consists of an electromagnet, a coil and a distance sensor. Figure 1 shows the basic principle where u_{RL} and i are the voltages and the current of the electromagnet with resistance R and inductance L, c is an unknown parameter, m is the mass of the coil and l is the distance between the electromagnet and the coil. From the second Newton law we can write

$$mg - F_m = m\,\frac{d^2 l}{dt^2}. \tag{1}$$

The magnetic force depends on the current i, the distance l, and the parameter c

$$F_m = c\,\frac{i^2}{l^2}. \tag{2}$$

The electric dynamic of the system is modeled by the following equation:

$$u_{RL}(t) = L\,\frac{di}{dt} + Ri. \tag{3}$$

The sensor and the actuator can be modeled with static functions where equation (4) is the model of the sensor and equation (5) is the model of the actuator

$$y = K_{\text{sens}} l + U_{\text{sens}}, \qquad K_{\text{sens}} = -4\left[\frac{V}{mm}\right], \qquad U_{\text{sens}} = 10[V]. \tag{4}$$

$$u = K_{\text{act}} u_{RL} + U_{\text{act}}, \qquad K_{\text{act}} = 2, \qquad U_{\text{act}} = -10[V]. \tag{5}$$

By using equations (1)–(3), the nonlinear unstable differential equation is obtained

$$\frac{Lm}{c}\left(g - \frac{d^2 l}{dt^2}\right)\frac{dl}{dt} - \frac{Lm}{2c}\,l\,\frac{d^3 l}{dt^3} + \frac{Rm}{c}\,l\left(g - \frac{d^2 l}{dt^2}\right) - u_{RL}\sqrt{\frac{m}{c}\left(g - \frac{d^2 l}{dt^2}\right)} = 0. \tag{6}$$

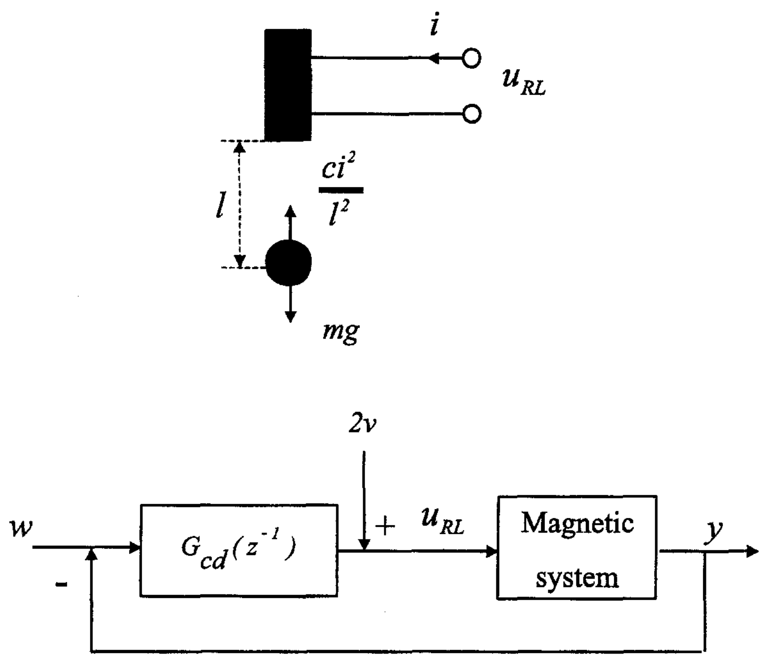

Figure 1. Closed loop magnetic suspension system.

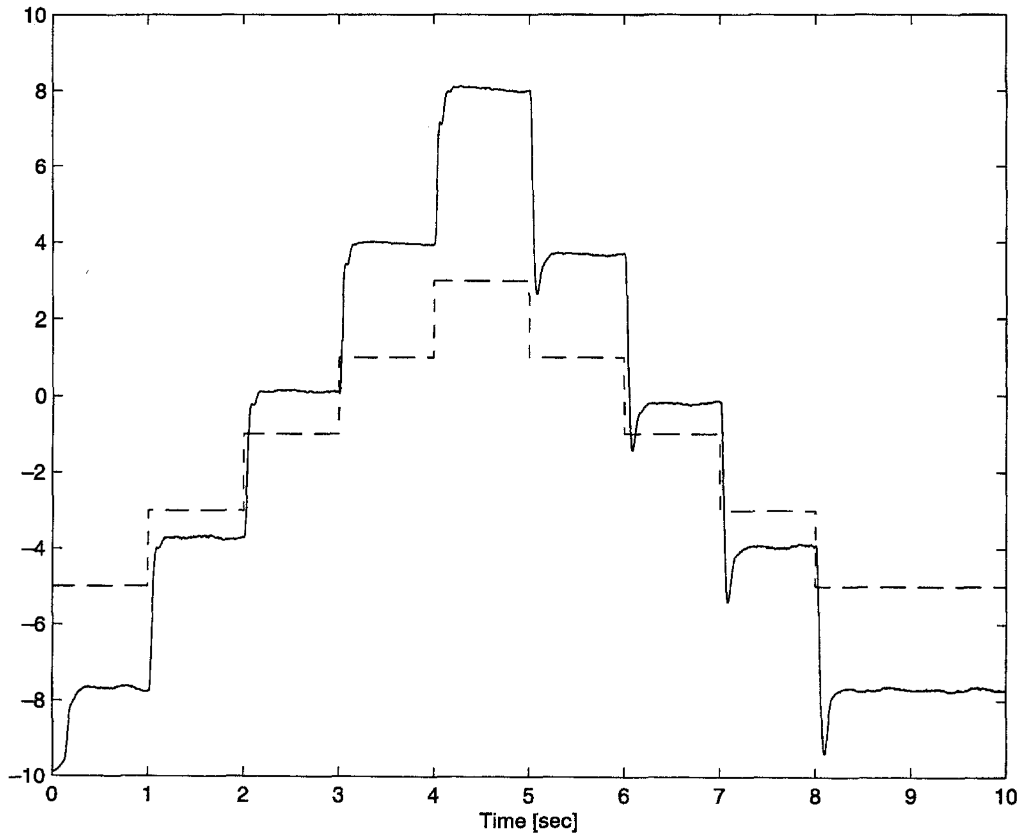

Figure 2. Dynamic response of the closed loop system: Reference (w): dotted, Output (y): solid.

It can be stabilized with the linear lead compensator with transfer function

$$G_{cc}(s) = 4.5\,\frac{(s+40)}{(s+400)}. \tag{7}$$

Using a sampling time of 2[ms], the discrete controller is as follows

$$G_{cd}\left(z^{-1}\right) = 4.5\,\frac{\left(1 - 0.09449z^{-1}\right)}{\left(1 - 0.4493z^{-1}\right)}. \tag{8}$$

Also the feedforward compensation of gravity of 2[v] was applied. Figure 1 shows the compensated system where w is the reference signal.

The lead compensator assures stability in the whole operating range. Figure 2 shows the dynamic behavior of the compensated system. It can be appreciated a considerable dynamic difference in the response when the reference signal is moving up or down. The system exhibits an undershoot when the reference signal is going down.

In the next sections, a nonlinear model of the closed loop system from w to y will be identified.

3. MODEL STRUCTURE

The proposed model structure used in this paper consists on a fuzzy global linear dynamic model (see Appendix A) followed by a piecewise linear (PWL) static function (see Appendix B). In some way, this model structure can be considered as a generalization of a Wiener model. The particular linear dynamic and nonlinear static technique used in a Wiener like structure is dictated by the characteristics of the specific system to be modeled. If the system exhibits a considerably oscillatory behavior, Kautz series is preferable over Laguerre series to cope the linear dynamic. In the present case, the magnetic system exhibits a dynamic behavior that cannot be properly approximated with any linear technique. The fuzzy global linear model can properly describe the unusual dynamic behaviors like the undershoot of the magnetic system described in the previous section. Then, the fuzzy model will be evaluated to describe the main dynamic behavior and the PWL function will approximate the static mapping between the output of the fuzzy model and the magnetic system output as well as the lower and upper bounds of this static gain. Different Wiener model identification approaches can be found in the relevant literature. A general classification of these approaches is the following.

- *The N-L Approach.* First, the output static nonlinearity is determined using steady-state data, then the dynamic linear block is identified, being the intermediate signal generated from the output signal using inverse nonlinearity mapping [10].
- *The L-N Approach.* First, the linear block is identified using a correlation technique; after that, the intermediate signal is generated from the input signal and finally the static nonlinearity is estimated [11].
- *The Simultaneous Approach.* Parameters of the linear block and the static nonlinearity are estimated at the same time. For example, [12,13] describe a prediction error based on simultaneous Wiener model identification procedure.

Even though, the model structure used in this paper is not a strict Wiener, the second identification approach is used because is straightforward and ensures an accurate description of the static nonlinearity.

4. MODELLING RESULTS

A PRBS input sequence is used for the identification of the fuzzy dynamic block using the global linear approach described in Appendix A. The TS model used has antecedent fuzzy sets A1 and A2 and are shown in Figure 3. They have been chosen in accordance with different process dynamic when process output is increasing or decreasing. Different dynamic can be appreciated from a series of step response shown in Figure 2.

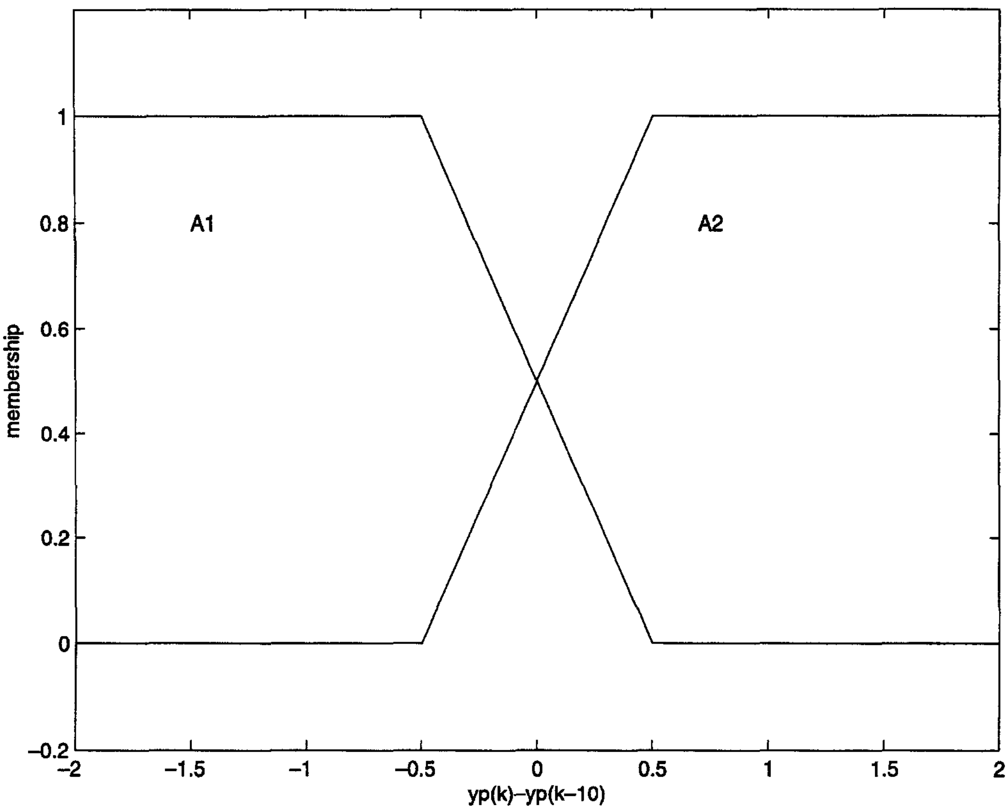

Figure 3. Antecedent fuzzy set for $y_p(k) - y_p(k-10)$.

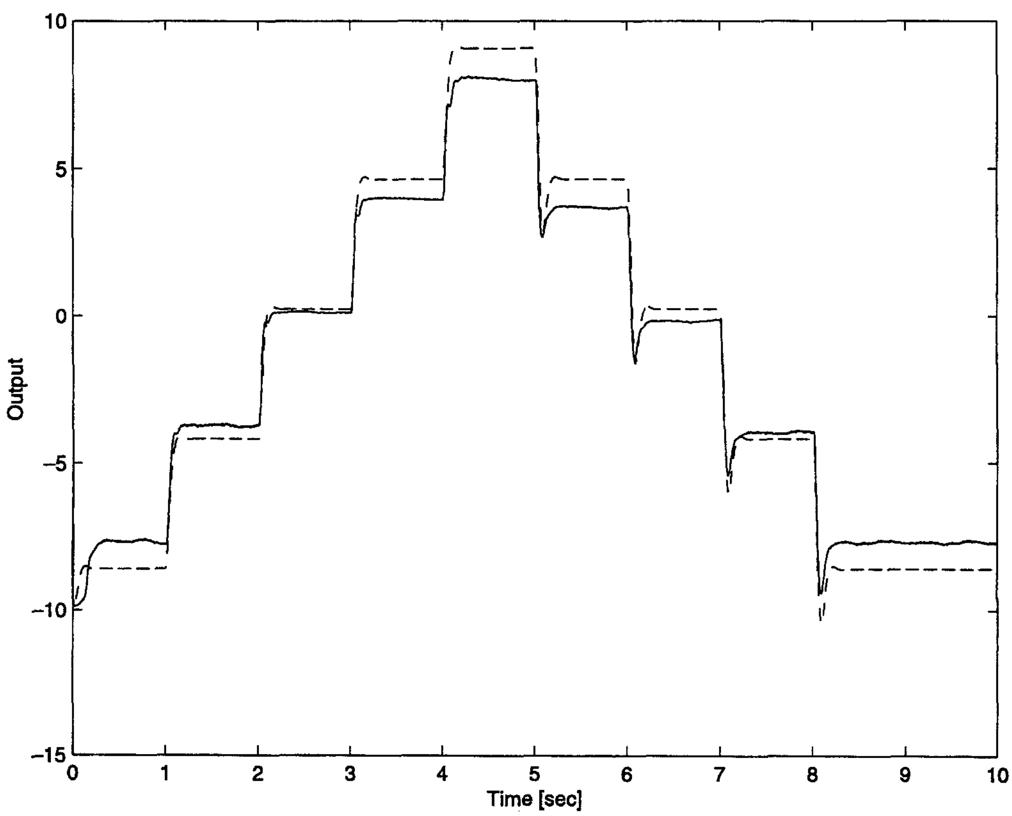

Figure 4. Dynamic response of the system (y: solid) and the fuzzy model (y_p: dashed).

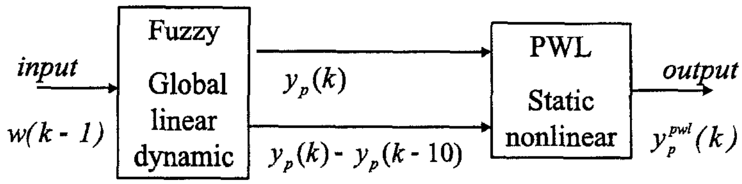

Figure 5. Model structure with $\mathbb{R}^2 \rightarrow \mathbb{R}^1$ PWL mapping.

The identified TS model with the sampling time of 2[ms] is

$$\begin{aligned} R^1 &: \text{if } y_p(k) - y_p(k-10) \text{ is A1, then} \\ y_p(k+1) &= 1.3449 y_p(k) + 0.2288 y_p(k-1) - 0.5822 y_p(k-2) \\ &\quad + 0.0188 w(k-2) + 0.0199 \end{aligned}$$

$$\begin{aligned} R^2 &: \text{if } y_p(k) - y_p(k-10) \text{ is A2, then} \\ y_p(k+1) &= 1.3174 y_p(k) + 0.1495 y_p(k-1) - 0.4755 y_p(k-2) \\ &\quad + 0.0189 w(k-2) + 0.0219 \end{aligned}$$

The response of this fuzzy model compared with the system output may be appreciated in Figure 4.

The toolbox [14] was used to identify the static PWL function. This toolbox allows not only to obtain a nominal model but also the uncertainty bands enclosing all the available data, as shown in Appendix B. In this way, a PWL description of the upper and lower bounds λ_l and λ_u can be evaluated. A complete description of the robust identification can be found in [15]. These bounds may also be used as indicators of the model quality. Different dynamic model alternatives may

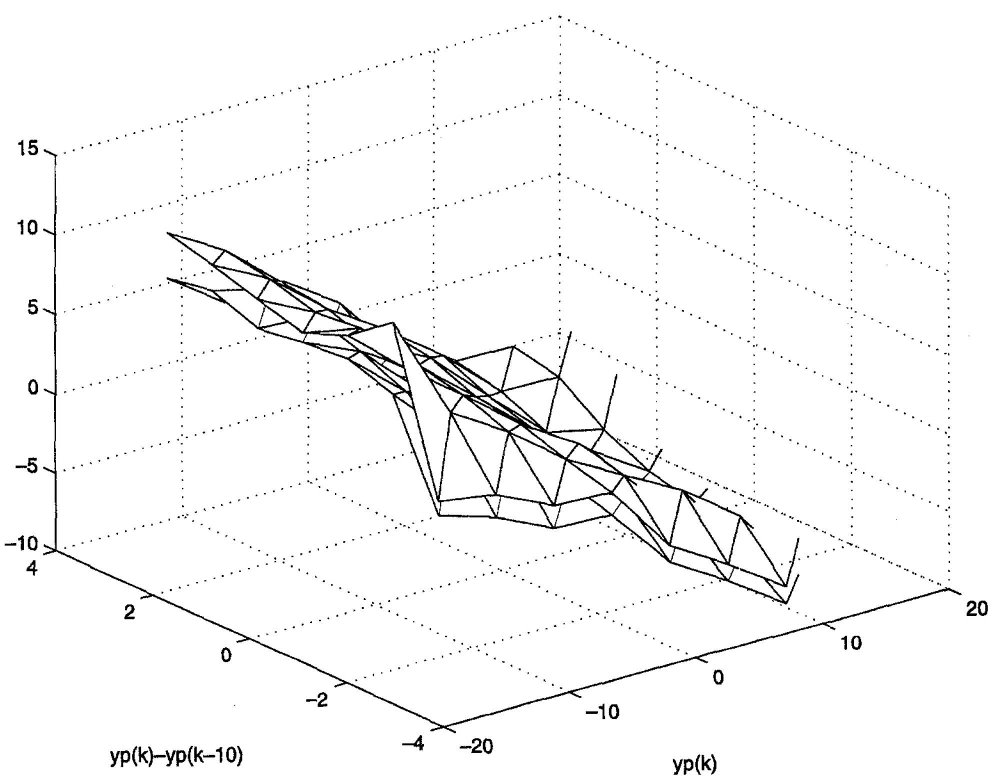

Figure 6. Upper and lower gain for the $y_p^{\mathrm{PWL}}(\mathbb{R}^2 \rightarrow \mathbb{R}^1)$ mapping.

be compared with these bounds. The dynamic model for which the narrow bounds are achieved minimizes the unmodeled dynamics. These bounds of the static nonlinear gain may also be used to evaluate the bounds of the dynamic response. In this paper, two alternative mappings were studied. First, a $\mathbb{R}^1 \to \mathbb{R}^1$ mapping was evaluated from the actual output of the fuzzy model to the actual system output and second a $\mathbb{R}^2 \to \mathbb{R}^1$ mapping from the actual and a delayed output of the fuzzy model to the actual output of the system. Figure 5 shows this model structure.

Figure 6 shows the upper and lower bounds of the $\mathbb{R}^2 \to \mathbb{R}^1$ PWL mapping.

To evaluate the performance of the uncertainty model, the mean of the dynamic uncertainty band over a validation set was computed. Table 1 summarizes the results concerning to the dynamic uncertainty using both mappings. It is clear that the second alternative considerably reduces the uncertainty bands.

Figure 7 shows the dynamic behavior of the model y_p^{PWL} compared to the system output y. In order to have a closer vision of the results, Figure 8 presents a zoom of the previous one. In these figures, the dynamic bands obtained from the robust approximation bounds of the static gain showed in Figure 6, may also be appreciated. Is clear that the dynamic evolution of the system is always inside these dynamic bounds.

A validation study was performed with data that has not been used in the approximation. Figure 9 shows a representative result. Several validation tests were performed and only in some very short periods of time a negligible drift outside these bounds could be appreciated.

Table 1.

Mapping	Input	Output	Mean of the Dynamic Uncertainty Band
$\mathbb{R}^1 \to \mathbb{R}^1$	$y_p(k)$	$y(k)$	2.2
$\mathbb{R}^1 \to \mathbb{R}^2$	$y_p(k)$, $y_p(k-10)$	$y(k)$	1.4

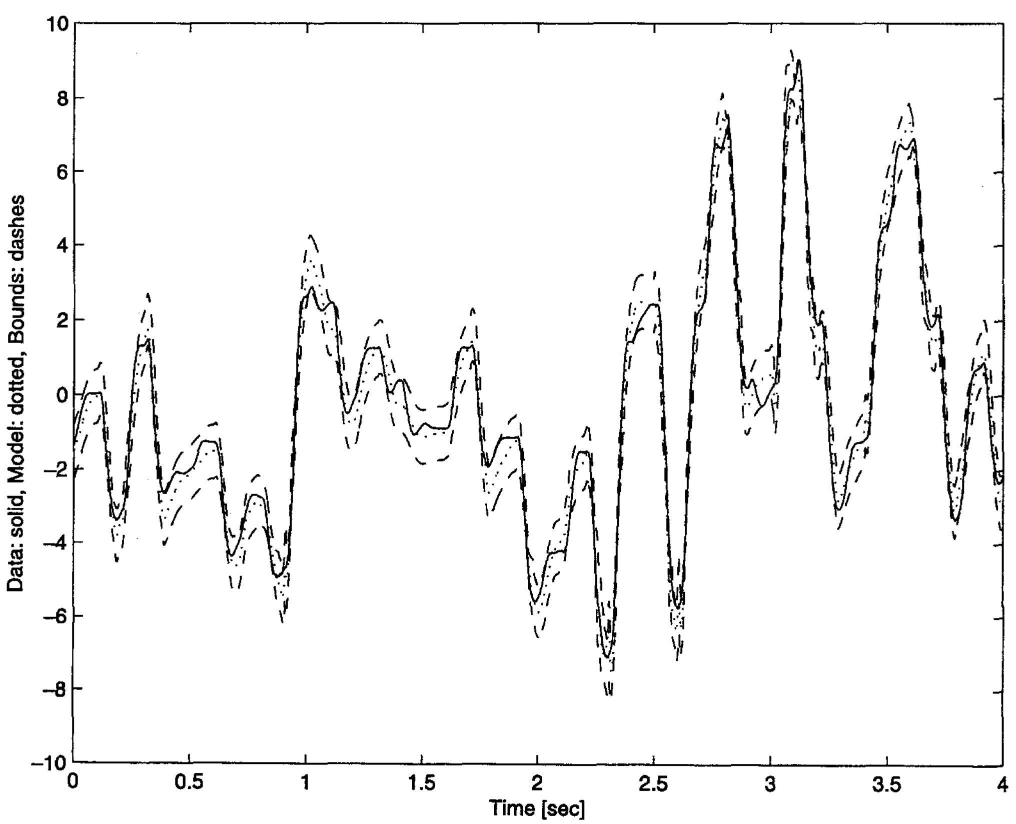

Figure 7. Approximation results. Magnetic system (y: solid) and FUZZY PWL model (y_p^{PWL}: dotted. Dynamic bounds: dashed).

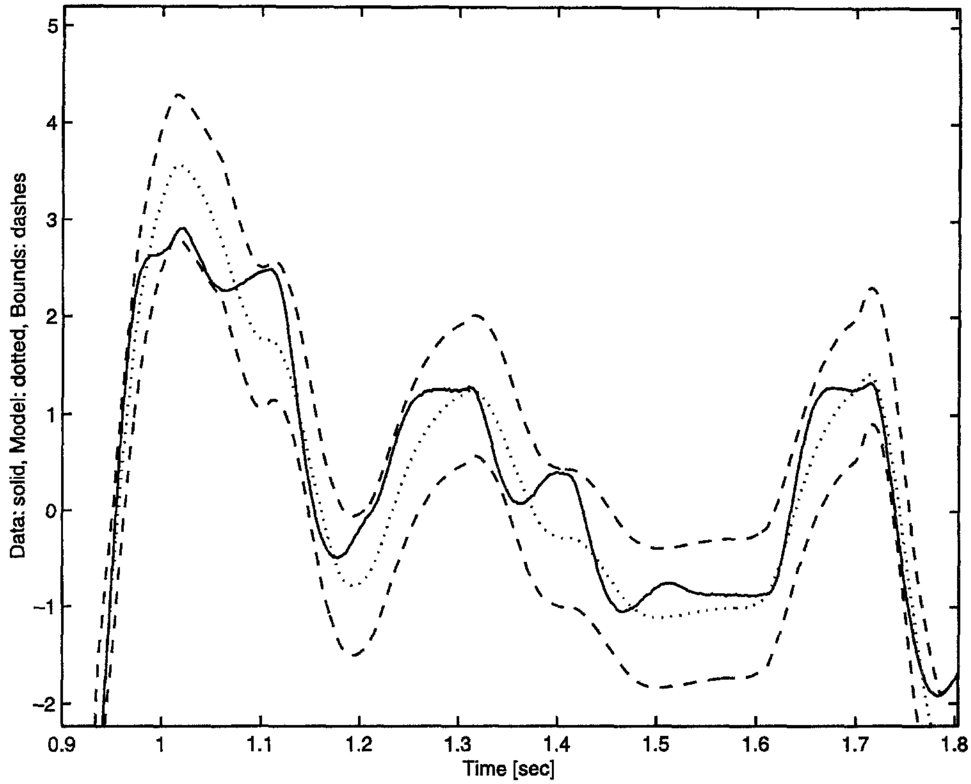

Figure 8. Approximation results. Magnetic system (y: solid) and FUZZY PWL model (y_p^{PWL}: dotted. Dynamic bounds: dashed).

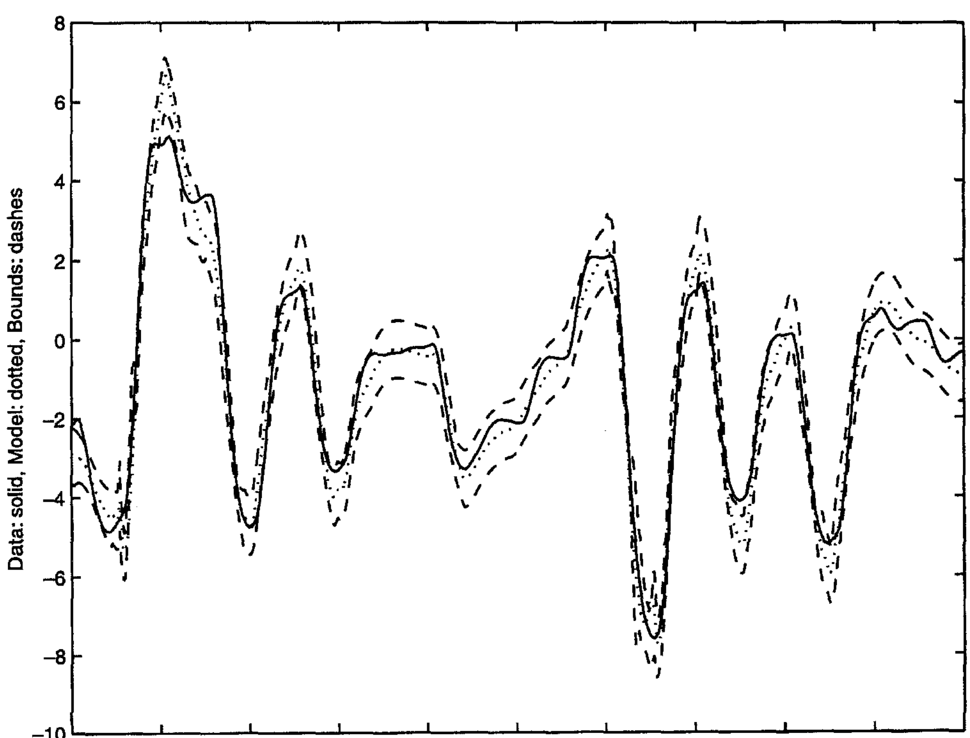

Figure 9. Validation results. Magnetic system (y: solid) and FUZZY PWL model (y_p^{PWL}: dotted. Dynamic bounds: dashed).

5. CONCLUSION

A fuzzy PWL structure for a nominal as well as uncertain model evaluation from input-output experimental data of a magnetic suspension system was presented. The system exhibits a particular behavior; it has an undershoot when the reference signal is going down. The model resembles a Wiener structure were a fuzzy global linear approach is used to describe the main dynamic characteristics and PWL functions describes the static nonlinearity and its uncertainty. The results show the viability of the proposed modelling technique. Several validation tests were performed and only in some very short periods of time a negligible drift outside these bounds could be appreciated. It is important to note that the PWL functions used have a simple VLSI electronic implementation. Then, it is possible to develop a real time implementation of this model structure for a large class of systems.

APPENDIX A
FUZZY IDENTIFICATION

Fuzzy models are, like neural networks, universal approximators. Originally, fuzzy models represent a static nonlinear function of input and output variables. The dynamical response is obtained with feeding in tap-delayed input variables and feeding back tap-delayed output variables. The most widely used type of fuzzy model in the Takagi-Sugeno (TS) [16] that can be written as follows

$$R^j : \text{if } x_1 \text{ is } A_1^j \text{ and } x_N \text{ is } A_N^j, \text{ then } y = f^j\left(x_1, \dots, x_N\right), \tag{9}$$

where x_i are inputs, A_i^j are subsets of the input space, y is the output and f^j is a function, generally nonlinear. In the present paper, a minor modification of the TS rule was made: the antecedent variable is not part of the regressor. For the third-order model, i^{th} rule can be written as

$$\begin{gathered} \mathrm{R}^i: \ \text{if } av \text{ is } \mathrm{A}^i, \text{ then} \\ y_p(k+1) = a_{1i}y_p(k) + a_{2i}y_p(k-1) + a_{3i}y_p(k-2) + b_i w(k-D) + r_i, \end{gathered} \tag{10}$$

where $y_p(k+1)$ is the output and $y_p(k)$, $y_p(k-1)$, $y_p(k-2)$, $w(k-D)$ are the inputs of the fuzzy model. D stands for the dead time expressed by the number of samples, A^i are antecedent fuzzy sets and av is the antecedent variable, in our case $\text{av} = y_p(k) - y_p(k-10)$.

Using Fuzzy mean defuzzification method, the output is expressed by the following equation:

$$y_p(k+1) = \sum_{i=1}^{K} \beta_i(k)\left(a_{1i}y_p(k) + a_{2i}y_p(k-1) + a_{3i}y_p(k-2) + b_i w(k-D) + r_i\right), \tag{11}$$

where K stands for the number of rules and $\beta_i(k)$ is the normalized degree of fulfillment of i^{th} rule at k^{th} step. For the purpose of identification, equation (11) can be written with K equation as follows [17]

$$\begin{aligned}
\beta_1(k)y_p(k+1) &= \beta_1(k)a_{11}y_p(k) + \beta_1(k)a_{21}y_p(k-1) \\
&\quad + \beta_1(k)a_{31}y_p(k-2) + \beta_1(k)b_1 w(k-D) + \beta_1(k)r_1, \\
&\ \vdots \\
\beta_i(k)y_p(k+1) &= \beta_i(k)a_{1i}y_p(k) + \beta_i(k)a_{2i}y_p(k-1) \\
&\quad + \beta_i(k)a_{3i}y_p(k-2) + \beta_i(k)b_i w(k-D) + \beta_i(k)r_i, \\
&\ \vdots \\
\beta_K(k)y_p(k+1) &= \beta_K(k)a_{1K}y_p(k) + \beta_K(k)a_{2K}y_p(k-1) \\
&\quad + \beta_K(k)a_{3K}y_p(k-2) + \beta_K(k)b_K w(k-D) + \beta_K(k)r_K,
\end{aligned} \tag{12}$$

To evaluate parameters a_{1i}, a_{2i}, a_{3i}, b_i, and r_i of the i^{th} rule, the regression matrix $\mathbf{\Psi}_i$ and the output data vector $\mathbf{Y}_p^i$ should be obtained as presented in the following equations

$$\psi_i(k) = [\beta_i(k)y_p(k) \quad \beta_i(k)y_p(k-1) \quad \beta_i(k)y_p(k-2) \quad \beta_i(k)w(k-D) \quad \beta_i(k)], \tag{13}$$

$$\mathbf{\Psi}_i = \begin{bmatrix} \psi_i(D) \\ \vdots \\ \psi_i(k) \\ \vdots \\ \psi_i(N-1) \end{bmatrix}, \tag{14}$$

$$\mathbf{Y}_p^i = \begin{bmatrix} \beta_i(D)y_p(D+1) \\ \vdots \\ \beta_i(k)y_p(k+1) \\ \vdots \\ \beta_i(N-1)y_p(N) \end{bmatrix}. \tag{15}$$

The vector of parameters of i^{th} rule, $\boldsymbol{\theta}_i$, is obtained by using the least square method

$$\boldsymbol{\theta}_i = \left(\mathbf{\Psi}_i^\top \mathbf{\Psi}_i\right)^{-1} \mathbf{\Psi}_i^\top \mathbf{Y}_p^i, \tag{16}$$

where

$$\boldsymbol{\theta}_i = [a_{1i} \quad a_{2i} \quad a_{3i} \quad b_i \quad r_i]. \tag{17}$$

The steps from equations (13)–(16) should be repeated for all rules. Vectors $\boldsymbol{\theta}_i$ can be joined into a matrix

$$\mathbf{\Theta} = [\boldsymbol{\theta}_1 \quad \boldsymbol{\theta}_2 \quad \cdots \quad \boldsymbol{\theta}_K], \tag{18}$$

where i^{th} column represents the parameter vector of i^{th} rule. The fuzzy model of equation 11 can be written in the following form, also called global linear model:

$$y_p(k+1) = \tilde{a}_1 y_p(k) + \tilde{a}_2 y_p(k-1) + \tilde{a}_3 y_p(k-2) + \tilde{b}w(k-D) + \tilde{r}(k), \tag{19}$$

where the parameters are

$$\begin{aligned} \tilde{a}_1(k) &= \sum_{i=1}^{K} \beta_i(k)\mathbf{\Theta}_{1i}, \\ \tilde{a}_2(k) &= \sum_{i=1}^{K} \beta_i(k)\mathbf{\Theta}_{2i}, \\ \tilde{a}_3(k) &= \sum_{i=1}^{K} \beta_i(k)\mathbf{\Theta}_{3i}, \\ \tilde{b}(k) &= \sum_{i=1}^{K} \beta_i(k)\mathbf{\Theta}_{4i}, \\ \tilde{r}(k) &= \sum_{i=1}^{K} \beta_i(k)\mathbf{\Theta}_{5i}. \end{aligned} \tag{20}$$

APPENDIX B

PWL FUNCTION APPROXIMATION

In [9] a representation for the family of all continuous PWL mappings defined over a simplicial partition of a domain in $\mathbb{R}^{m_o}$ was proposed. This representation allows to uniformly approximate any Lipschitz continuous function defined on a compact domain. Julián [18] formulated the canonical expression for all the family of the PWL continuous functions defined over a simplicial partition of the domain

$$D = \{(v_1, \dots, v_{m_o}) : 0 \le v_i \le m_i\delta,\ i \in \{1, \dots, n\}\} \subset \mathbb{R}^{m_o},$$

where δ is the grid size and $m_i \in \mathbb{Z}_+$. This type of partition divides the domain D in simplices $\bar{S}^{(i)}$, $i = 1, 2, \dots, q$ such that $D = \bigcup_{i=1}^{q} \bar{S}^{(i)}$. The corresponding set of vertices for these simplices is called $V^{(i)}$. For simplicity, let us suppose that the domain D belongs to $\mathbb{R}^2$. If one function value is associated to each vertex, as illustrated by Figure 10, then it is possible to define a PWL function with the following characteristics.

1. The function values assigned to each vertex define a unique (and local) linear affine function for each simplex.
2. The local linear expressions defines a PWL continuous function because they are continuous on the boundaries of the partition.

The extension of this idea to a m_o-dimensional domain lead to define simplices of $m_o + 1$ vertices.

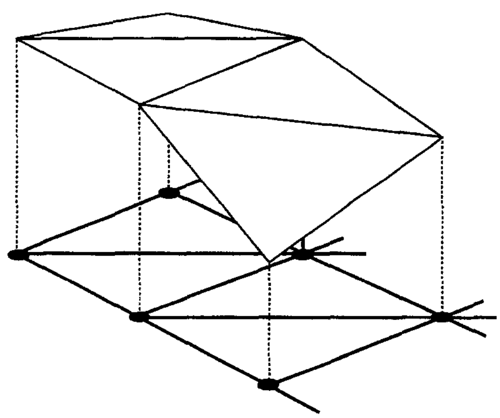

Figure 10. PWL function in $\mathbb{R}^2$.

Let $\mathrm{PWL}_H[D]$ the set of all the PWL continuous mappings with domain D partitioned with a given boundary configuration H. A basis of $\mathrm{PWL}_H[D]$ was constructed by defining each element of the basis as a function of k-nesting absolute value functions. The elements of this basis can be expressed in vector form as

$$\Lambda = \left[\Lambda^{0^\top}, \Lambda^{1^\top} \dots, \Lambda^{m_o^\top}\right]^\top,$$

ordered according to its nesting level (n.l.), where Λ^i is the vector containing the functions having n.l. $= i$. Then any function $h \in \mathrm{PWL}_H[D]$ can be written as

$$h(v) = E^\top \Lambda(v),$$

where $E = [E_0^\top, E_1^\top, \dots, E_{m_o}^\top]^\top$, and every vector E_i is a parameter vector associated to the vector function Λ^i.

Robust Approximation

Let us assume that the measure to be approximated has a given level of uncertainty in the form

$$\Im = \left\{h : D \mapsto R^1 : h(v) = h_N(v) + \Delta(v)\right\},$$

where h_N is a nominal function and Δ satisfies $\sup_{x\in D} \|\Delta(v)\| \le K$.

In addition, let us consider that a set $F = \{h_1, h_2, h_3, \dots, h_m\}$ of m measured values (members of $\Im$) over a set of points $X = \{v_1, v_2, v_3, \dots, v_m\}$ is available (i.e., $h_i = h(v_i)$, with $h \in \Im$ and $v_i \in X \subset D$).

We search an "upper" function h_u and a "lower" function h_l both belonging to $\mathrm{PWL}_H[D]$, satisfying

$$h_l(v_i) \le h(v_i) \le h_u(v_i), \qquad \forall\, v_i \in D,$$

to characterize the uncertainty function, in the sense that

$$h(v_i) = \alpha h_l(v_i) + (1-\alpha) h_u(v_i),$$

$\forall\, v_i \in X, h \in \Im$, where $0 \le \alpha \le 1$. In addition, it is also desirable that the band defined by these two functions be as narrow as possible. This is equivalent to find two functions h_u and h_l that solve the following optimization problems.

PROBLEM 1.

$$\min_{h_l \in \mathrm{PWL}_H[D]} \left(\max_{v_i \in X} \{|h_i - h_l(v_i)|\} \right), \tag{21}$$

s.t.,

$$h_i - h_l(v_i) \ge 0, \qquad \forall\, v_i \in X.$$

PROBLEM 2.

$$\min_{h_u \in \mathrm{PWL}_H[D]} \left(\max_{v_i \in X} \{|h_i - h_u(v_i)|\} \right), \tag{22}$$

s.t.,

$$h_u(v_i) - h_i \ge 0, \qquad \forall\, v_i \in X.$$

As h_u and $h_l \in \mathrm{PWL}_H[D]$ then they can be written as $h_l(v) = E_l^\top \Lambda(v)$ and $h_u(v) = E_u^\top \Lambda(v)$. It can be proved that the solution to these problems can be found as solutions of two linear programming problems, as stated in the following lemma.

LEMMA 1. *Let X, F, H, and D as described above. Problems (21) and (22) can be stated as the linear programming problems*

(1) $\min \lambda_l$ *subject to*

$$\begin{aligned} -c_l^\top \Lambda(v_i) - \lambda_l &\le -h_i, \qquad &\forall\, v_i \in X,\\ -c_l^\top \Lambda(v_i) &\ge -h_i, \qquad &\forall\, v_i \in X,\\ \lambda_l &\ge 0; \end{aligned}$$

(2) $\min \lambda_u$ *subject to*

$$\begin{aligned} c_u^\top \Lambda(v_i) - \lambda_u &\le h_i, \qquad &\forall\, v_i \in X,\\ c_u^\top \Lambda(v_i) &\ge h_i, \qquad &\forall\, v_i \in X,\\ \lambda_u &\ge 0; \end{aligned}$$

on the parameters E_l, E_u, λ_l, and λ_u.

PROOF. See [9]. ∎

REFERENCES

1. J.A.K. Suykens and J. Vandewalle, Editors, *Nonlinear Modeling*, Kluwer Academic, (1998).
2. M.J. Korenberg and L.D. Paarmann, Orthogonal approaches to time-series analysis and system identification, *IEEE Signal Processing Magazine* **29**.
3. M.A. Vázquez and O. Agamennoni, Approximate models for nonlinear dynamical systems and its generalization properties, *Mathl. Comput. Modelling* **33** (8/9), 965–986, (2001).
4. L. Castro, P. Julian, O. Agamennoni and A. Desages, Wiener modelling using canonical piecewise linear functions, *Latin American Applied Research Journal* **29**, **Nro.**, 265–272, (1999).

5. L. Castro, O. Agamennoni, C. D'Attellis, Rational wavelets in Wiener-like modelling, *Mathl. Comput. Modelling* **35** (9/10), 991–1006, (2002).
6. G. Sentoni, O. Agamennoni and J. Romagnoli, On the evaluation of a certain kind of approximation structure, *Latin American Applied Research Journal* **25/S**, 35–40, (1995).
7. G. Sentoni, O. Agamennoni, A. Desages and J. Romagnoli, Approximate models for nonlinear process control, *AIChE Journal* **42** (8), 2240–2250, (1996).
8. M. Lepetic, I. Škrjanc, H. Chiacchiarini and D. Matko, Predictive functional control based on fuzzy model: Comparison with linear predictive functional control and pid control, *Journal of Intelligent and Robotic Systems* **36**, 467–480, (2003).
9. P. Julián, A. Desages and O. Agamennoni, High level canonical piecewise linear representation using a simplicial partition, *IEEE Transactions on Circuits and Systems I* **46**, 463–480, (1999).
10. S. Gerksic, D. Juricić, S. Strmcnik and M. Matko, Wiener model based nonlinear predictive control, *International Journal of Systems Science* **31**, 189–202, (2000).
11. D. Westwick, M. Verhaegen, Identifying MIMO Wiener systems using subspace model identification methods, *Signal Processing* **52**, 235–258, (1996).
12. A. Kalafatis, N. Arifin, L. Wang and W. Cluett, A new approach to the identification of ph processes based on the Wiener model, Chemical Engineering Science **50**, 3693–3701, (1995).
13. T. Wigren, Recursive prediction error identification using the nonlinear Wiener model, *Automatica* **29**, 1011–1026, (1993).
14. P. Julián, *A Toolbox for the Piecewise Linear Approximation of Multidimensional Functions*, `http://www.pedrojulian.com`, (2000).
15. P. Julián and O. Agamennoni, Tools for the PWL approximation of continuous functions, In *Modern Applied Mathematics Techniques in Circuits*, (Edited by N.E. Mastorakis), pp. 199–204, Systems and Control, Hellenic Naval Academy, (1999).
16. K.M. Passino and S. Yurkovich, *Fuzzy Control*, Addison-Wesley, (1998).
17. I. Škrjanc and D. Matko, Predictive functional control based on fuzzy model for heat exchanger pilot plant, *IEEE Transactions on Fuzzy Systems* **8** (6), 705–712, (2000).
18. P. Julián, High level canonical piecewise linear representation: Theory and applications, Tesis Doctoral en Control de Sistemas, DIEC-Universidad Nacional del Sur, Bahía Blanca, Buenos Aires, Argentina, (1999).